Biophysical Journal, Volume *117*

Supplemental Information

Polyphosphate Initiates Tau Aggregation through Intra- and Intermolecular Scaffolding

Sanjula P. Wickramasinghe, Justine Lempart, Hope E. Merens, Jacob Murphy, Philipp Huettemann, Ursula Jakob, and Elizabeth Rhoades

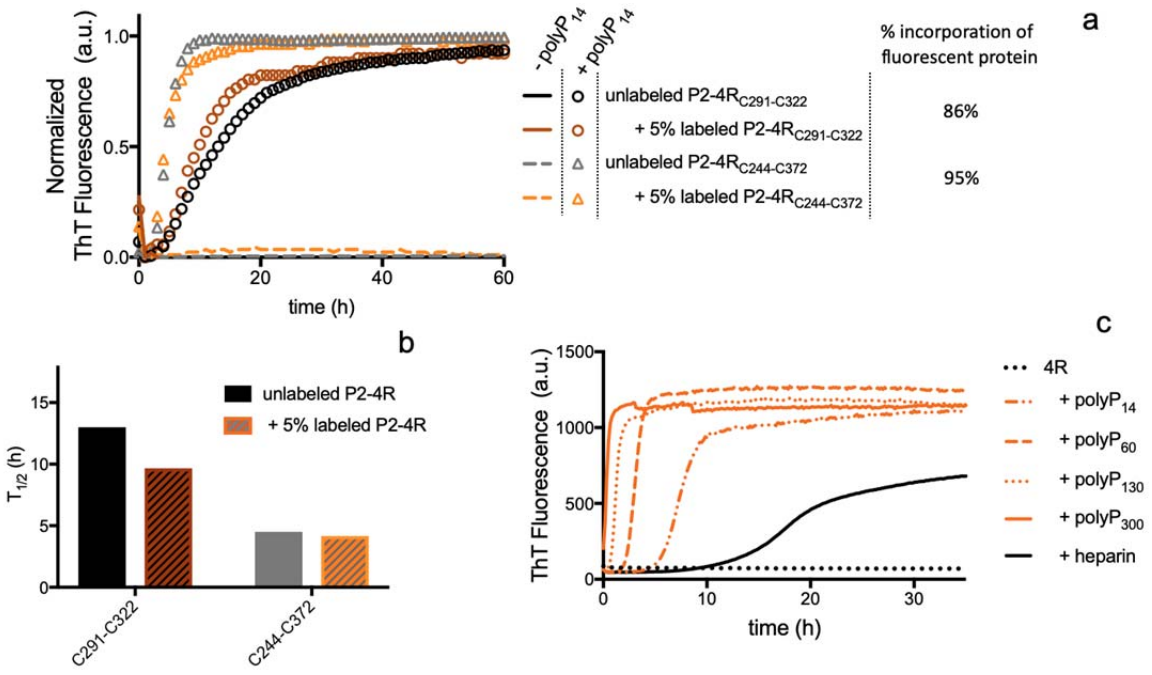

Figure S1. Labeled tau is incorporated into aggregates. Representative kinetic traces of ensemble aggregation measurements made using 100% unlabeled tau (black and gray) and 95 % unlabeled ta/5% fluorescently labeled tau (dark and light orange) in the absence or presence of 1 mM $polyP_{14}$ are shown (a). The incorporation of fluorescent into the aggregates is confirmed as described in the *Materials and Methods*. Kinetics were quantified by $T_{1/2}$ (b). These experiments were carried out twice to ensure reproducibility. Representative kinetic traces of 4R aggregation as measured by an increase in Thioflavin T fluorescence for 25 µM tau with 1 mM polyP or 18 µM heparin (c).

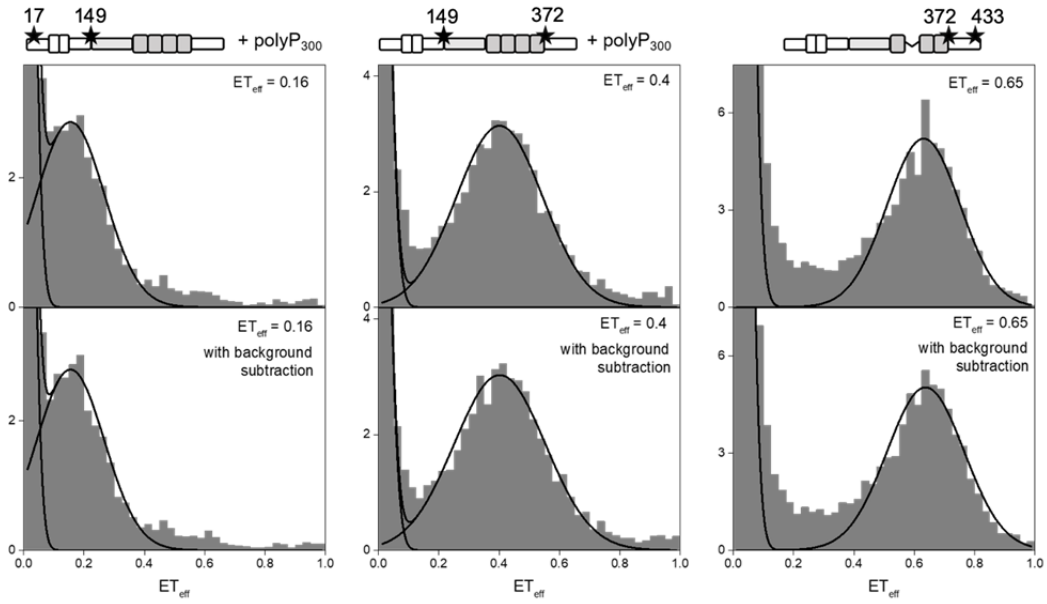

Figure S2. ET_{eff} histograms without and with background subtraction. ET_{eff} histograms for three different tau constructs without (upper) and with (lower) subtracting the average background signal from the individual events prior to calculating ET_{eff} as described in the *Materials & Methods*.

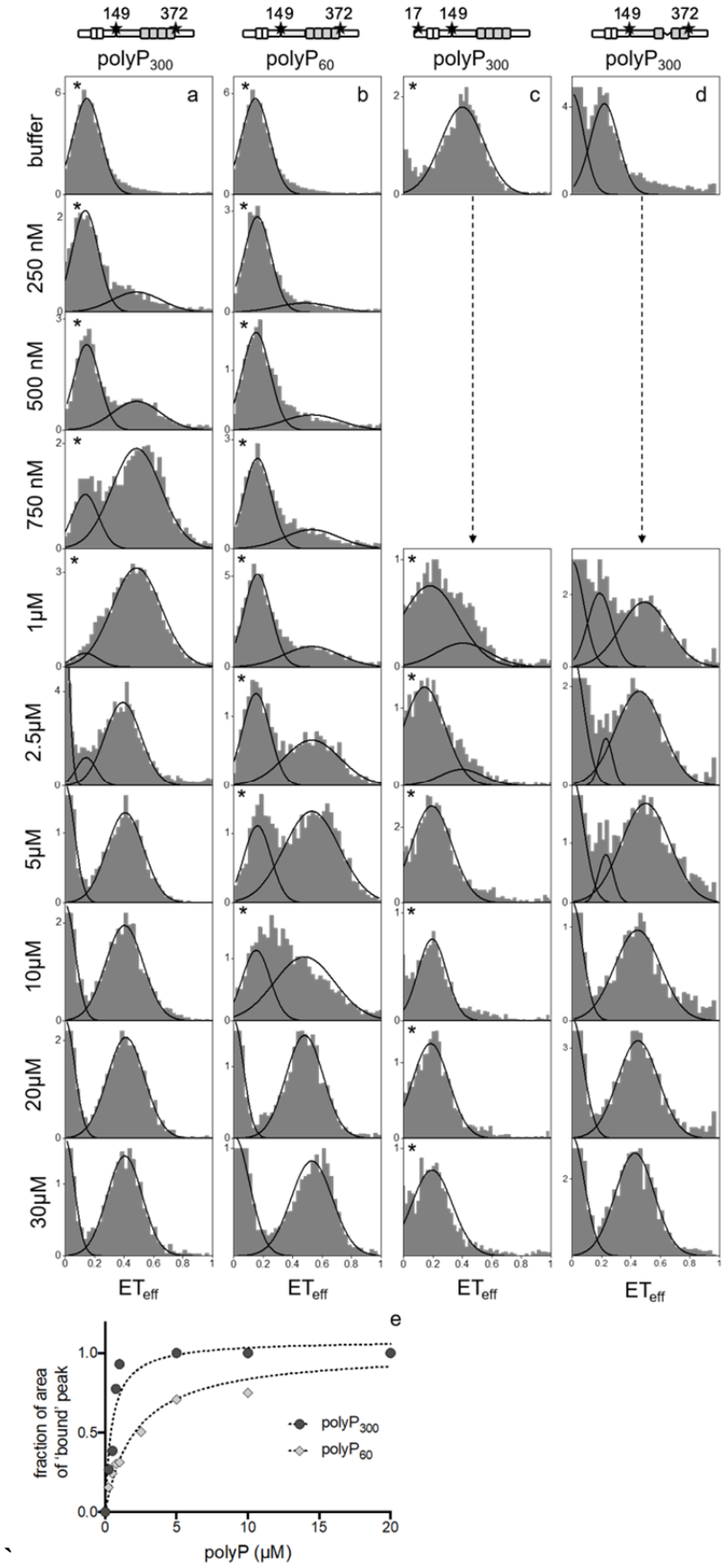
149 372
149 372
17 149
149 372
polyP300
polyP60
polyP300
polyP300
a
b
c
d
buffer
250 nM
500 nM
750 nM
1μM
2.5μM
5μM
10μM
20μM
30μM
ETeff
ETeff
ETeff
ETeff
e
fraction of area of 'bound' peak
polyP300
polyP60
polyP (μM)

Figure S3. ET_{eff} histograms as a function of polyP concentration. SmFRET measurements were made for 2N4R $tau_{C149\text{-}C372}$ with $polyP_{300}$ (a) or $polyP_{60}$ (b), $tau_{C17\text{-}C149}$ with $polyP_{300}$ (c) and 2N3R $tau_{C149\text{-}C372}$ with $polyP_{300}$ (d). PolyP concentrations ranged from 0 (top row) to 30 μM (bottom row). All histograms converged to single peaks before or at 20 μM polyP and no significant shifts in ET_{eff} were observed at higher concentrations of polyP. For calculation of binding curves, the center for the bound and unbound peaks were determined at limiting concentrations and fixed for intermediate concentrations when possible. Note that at high polyP concentrations (i.e. 20 μM) the polyP-bound peak is shifted from the polyP-bound peak at lower polyp concentrations (i.e. 20 μM). This likely reflects low affinity interactions between tau and polyP, as seen previously with heparin. The fraction of tau with polyP-bound (e) is calculated as the area of the bound peak over the total area of the bound and unbound peaks. These curves are fit with a hyperbolic binding equation to yield approximate K_D's for $polyP_{300}$ (~0.4 μM monomer or 1.3 nM chain) and $polyP_{60}$ (~2 μM or 33 nM chain). An asterisk in the left hand corner of a panel indicates the measurement was made using PIE-FRET.

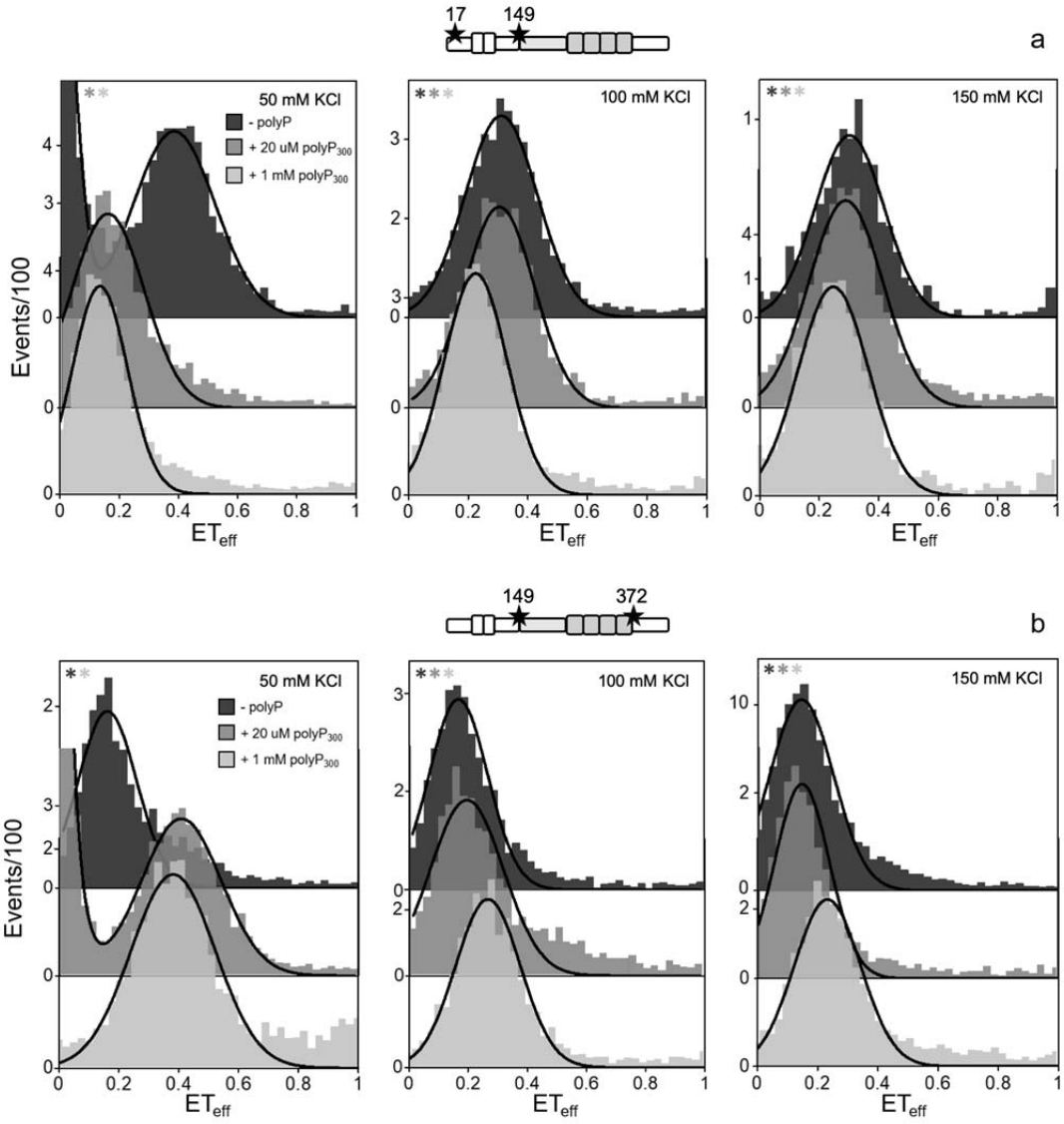

Figure S4. ET_{eff} histograms in the presence of polyP and increased KCl SmFRET measurements were made for 2N4R $tau_{C17\text{-}C149}$ (a) and $tau_{C149\text{-}C372}$ (b) with 50mM (left column), 100 mM (middle column) and 150 mM (right column) KCl in the absence of polyP (top row) and with the addition of 20 μM (middle row) and 1 M $polyP_{300}$ (bottom row. While 20 μM polyP causes only small changes in the histograms at higher salt concentrations, the polyP-bound peak is populated 1 M $polyP_{300}$ for both 100 mM and 150 mM KCl An asterisk in the left hand corner of a panel indicates the measurement was made using PIE-FRET.

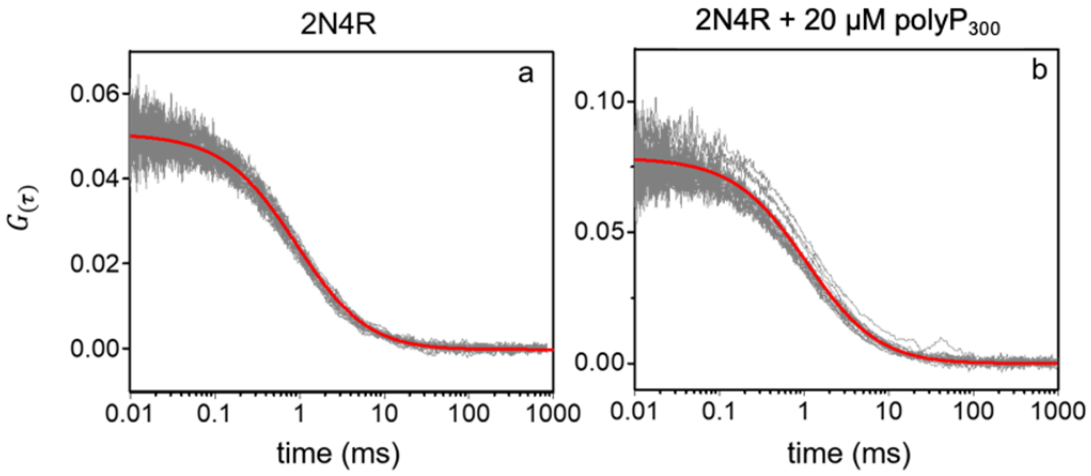

Figure S5. Representative autocorrelation curves measured by FCS. Shown are 25 individual autocorrelation curves of 10 seconds each (gray) along with the fit to the averaged curve (red) for 20 nM 2N4R tau in the absence (a) or presence (b) of 20 µM $polyP_{300}$.

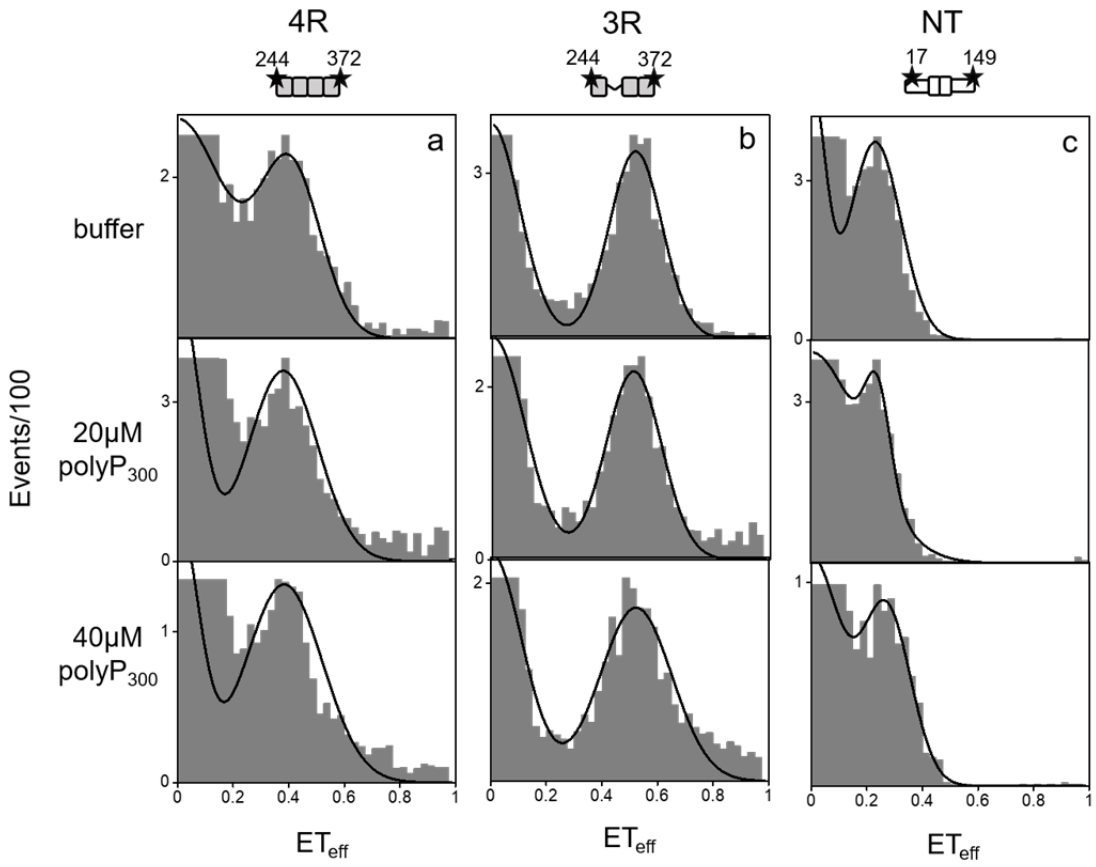

Figure S6. PolyP does not cause conformational changes in the MTBR and N-terminal fragments. Histograms measured by smFRET of $4R_{C244\text{-}C372}$ (a), $3R_{C244\text{-}C372}$ (b) and $NT_{C17\text{-}C149}$ (c) in the absence (upper row) and presence of 20 μM (center row) or 40 μM (lower row) $polyP_{300}$. The higher polyP concentration was tested to determine whether weak binding occurs in either of these regions. No changes to the histograms are observed for these fragments even at the higher polyP concentration.

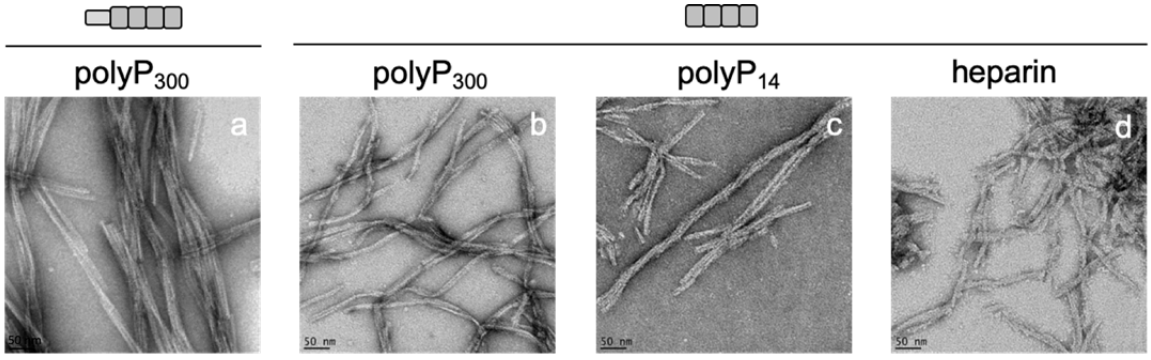

Figure S7. TEM images of tau-polyP fibers. Images of P2-4R with $polyP_{300}$ (a) and 4R with $polyP_{300}$ (b), $polyP_{14}$ (c) and heparin (d).

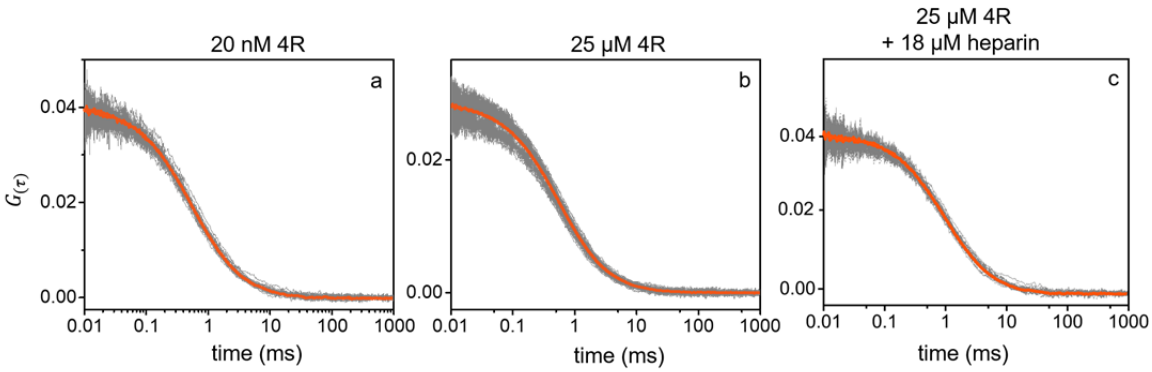

Figure S8. PolyP is required for crosslinking of tau. Autocorrelation curves of 20 nM labeled 4R in the absence (a) or presence (b) of 25 µM unlabeled 4R or (c) 25 µM unlabeled 4R and 18 µM heparin. Fits of the averaged curves yield comparable diffusion times, despite the 1000x difference in tau concentration.

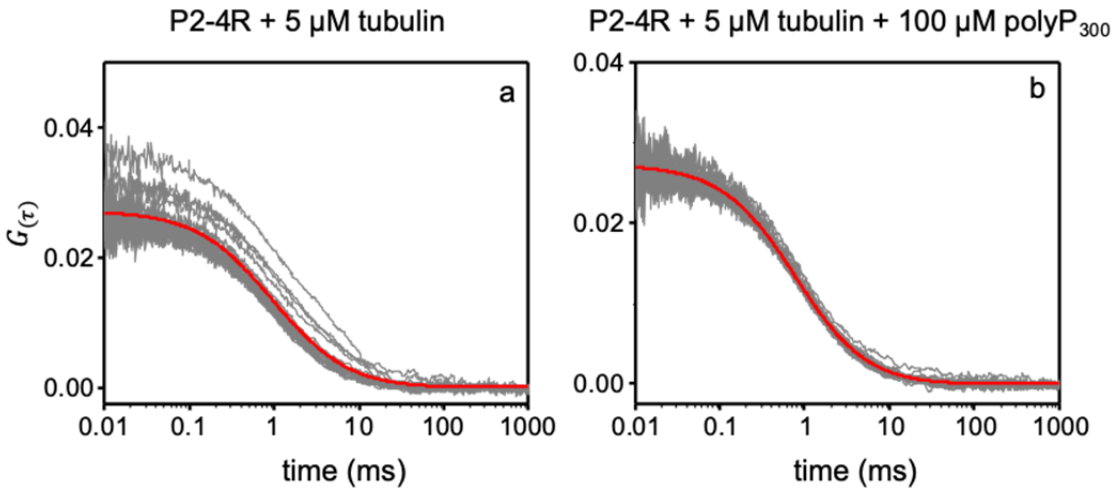

Figure S9. Autocorrelation curves of P2-4R with tubulin and polyP$_{300}$.

Autocorrelation curves of P2-4R and 5 µM tubulin in the absence (a) or presence (b) of 100 µM polyP$_{300}$.

labeling positions	construct	ET_{eff} (buffer)	ET_{eff} (+ $polyP_{300}$)	ΔET_{eff}
C17-C433	2N4R	0.15 ± 0.004	0.09 ± 0.004	-0.06 ± 0.006
	2N3R	0.18 ± 0.002	0.11 ± 0.006	-0.07 ± 0.006
C17-C149	2N4R	0.40 ± 0.01	0.18 ± 0.003	-0.22 ± 0.010
	2N3R	0.40 ± 0.004	0.21 ± 0.005	-0.19 ± 0.006
C149-C372	2N4R	0.17 ± 0.005	0.40 ± 0.002	0.23 ± 0.005
	2N3R	0.19 ± 0.002	0.44 ± 0.009	0.25 ± 0.009
C372-C433	2N4R	0.69 ± 0.003	0.50 ± 0.006	-0.19 ± 0.007
	2N3R	0.66 ± 0.002	0.46 ± 0.006	-0.20 ± 0.006

Table S1. Mean ET_{eff} values for 2N3R and 2N4R tau in the absence and presence of 20 µM $polyP_{300}$. Mean ET_{eff} and s.e.m. calculated for a minimum of three measurements with and without the addition of polyP. ΔET_{eff} is the difference between tau+$polyP_{300}$ and tau. Error of ΔET_{eff} is calculated by propagation of error as described in the *Materials and Methods*. Representative histograms are shown in Fig. 2.

	diffusion time (μs)		
	buffer	$polyP_{300}$	$polyP_{14}$
2N4R	925 ± 1	1055 ± 5.6	940 ± 3.3
P2-4R	628 ± 8.5	763 ± 3.3	672 ± 5
4R	534 ± 1.0	617 ± 1.0	566 ± 1.2
2N3R	909 ± 12.0	1056 ± 10.2	941 ± 1.3
P2-3R	430 ± 10.0	504 ± 12.7	450 ± 7.0
3R	377 ± 2.5	417 ± 1.4	390 ± 5.3
P1P2	482 ± 4.3	581 ± 2.2	502 ± 11.3
NT	585 ± 0.7	592 ± 8	585 ± 3.0
aSyn*	550	550	

Table S2. Mean diffusion times of tau constructs in the absence and presence of $polyP_{300}$ or $polyP_{14}$. Mean diffusion time and s.e.m. calculated from three independent sets of measurements. The percent change in diffusion time with the addition of polyP is shown in Fig. 3. aSyn was only measured once as a control.

labeling positions	construct	ET_{eff} (buffer)	ET_{eff} (+ $polyP_{300}$)	ΔET_{eff}
C244-C372	2N4R	0.29 ± 0.008	0.51 ± 0.002	0.22 ± 0.008
	P2-4R	0.31 ± 0.002	0.43 ± 0.003	0.12 ± 0.004
	4R	0.39 ± 0.004	0.39 ± 0.016	0 ± 0.016
C244-C372	2N3R	0.40 ± 0.002	0.59 ± 0.001	0.19 ± 0.002
	P2-3R	0.44 ± 0.006	0.50 ± 0.006	0.07 ± 0.008
	3R	0.51 ± 0.006	0.50 ± 0.006	-0.01 ± 0.008
C149-C244	2N4R	0.35 ± 0.005	0.50 ± 0.002	0.15 ± 0.005
	2N3R	0.36 ± 0.005	0.54 ± 0.005	0.18 ± 0.007
	PRR	0.39 ± 0.006	0.47 ± 0.007	0.07 ± 0.009
C17-C149	2N4R	0.40 ± 0.01	0.18 ± 0.003	-0.22 ± 0.010
	2N3R	0.40 ± 0.004	0.21 ± 0.005	-0.19 ± 0.006
	NT	0.23 ± 0.014	0.23 ± 0.015	0 ± 0.021

Table S3. Mean ET_{eff} for tau constructs in the absence and presence of $polyP_{300}$.

Mean ET_{eff} and s.e.m calculated for a minimum of three measurements with and without the addition of polyP. ΔET_{eff} is the difference between tau+$polyP_{300}$ and tau. Error of ΔET_{eff} is calculated by propagation of error as described in the *Materials and Methods*. Representative histograms for the different conditions are show in Fig. 4 and Fig. S6.

labeling positions	ET_{eff} (buffer)	polyP	ET_{eff} (+polyP)	ΔET_{eff}
C17-C149	0.40 ± 0.01	$polyP_{300}$	0.18 ± 0.003	-0.22 ± 0.010
		$polyP_{130}$	0.20 ± 0.004	-0.20 ± 0.011
		$polyP_{60}$	0.23 ± 0.009	-0.17 ± 0.013
		$polyP_{14}$	0.40 ± 0.013	0 ± 0.016
C149-C372	0.17 ± 0.005	$polyP_{300}$	0.40 ± 0.001	0.23 ± 0.005
		$polyP_{130}$	0.40 ± 0.004	0.23 ± 0.006
		$polyP_{60}$	0.48 ± 0.01	0.35 ± 0.011
		$polyP_{14}$	0.18 ± 0.029	0.01 ± 0.029

Table S4. Mean ET_{eff} of 2N4R tau in the absence and presence of different chain lengths of polyP. Mean ET_{eff} and s.e.m. calculated for a minimum of three measurements with and without the addition of polyP. ΔET_{eff} is the difference between tau+polyP and tau. Error of ΔET_{eff} is calculated by propagation of error as described in the *Materials and Methods*. Representative histograms of the different polyP chain lengths are shown in in Fig 5.

	$T_{1/2}$ (h)				
construct	$polyP_{300}$	$polyP_{130}$	$polyP_{60}$	$polyP_{14}$	heparin
4R	0.4 ± 0.04	1.2 ± 0.07	3.4 ± 0.11	6.6 ± 0.51	15.5 ± 1.74
3R	4.3 ± 1.26	6.8 ± 1.07	30.3 ± 3.95	44.1 ± 3.2	67.2 ± 4.63

	$T_{1/2}$ (h)			
construct	P2-4R	P2-3R	4R	3R
$polyP_{300}$	0.3 ± 0.12	1.0 ± 0.32*	0.4 ± 0.03*	4.3 ± 0.80*
$polyP_{14}$	8.0 ± 0.65	25.1 ± 2.33	7.2 ± 0.35	42.3 ± 2.32

Table S5. Aggregation half-times ($T_{1/2}$). Mean $T_{1/2}$ and s.e.m. from ensemble experiments using ThT fluorescence to follow aggregation kinetics. For the $polyP_{300}$ data, differences in the $T_{1/2}$ of 3R as compared to 4R, P2-3R and P2-4R are statistically significant (denoted by *) with p-values of 0.0007, 0.004 and 0.003 respectively. Table contains $T_{1/2}$ times shown in Fig 6.

labeling positions	ET_{eff} (buffer)	heparin (μM)	ET_{eff} (+ heparin)	ΔET_{eff}
C17-C149	0.40 ± 0.01	0.13	0.24 ± 0.003	-0.16 ± 0.010
		1.75	0.24 ± 0.003	-0.16 ± 0.010
C149-C372	0.17 ± 0.005	0.13	0.36 ± 0.001	0.19 ± 0.005
		1.75	0.35 ± 0.006	0.18 ± 0.008

Table S6. Mean ET_{eff} of 2N4R tau in the absence and presence of heparin. Mean ET_{eff} and s.e.m. calculated for a minimum of three measurements without and with the addition of heparin. ΔET_{eff} is the difference between tau+heparin and tau. Error of ΔET_{eff} is calculated by propagation of error as described in the *Materials and Methods*. Representative histograms are shown in Fig 7.

Supporting References

1. Elbaum-Garfinkle, S., and E. Rhoades. 2012. Identification of an aggregation-prone structure of tau. J Am Chem Soc. 134:16607-16613.